Application of Asymptotic Waveform Evaluation for Emc Analysis of Electrical Interconnects

W. T. Smith, S. K. Das
Department of Electrical Engineering
University of Kentucky
Lexington, Kentucky

Abstract:

Asymptotic Waveform Evaluation (AWE) is a recently developed technique for time-domain analysis of electrical interconnects. AWE is an approximate method whose accuracy depends on the order of the approximation. In this paper, asymptotic waveform evaluation is used to analyze various transmission line-type interconnects. The principal problem addressed is evaluation of crosstalk. AWE is applied to a variety of circuits including a lumped-pi model, a transmission line model and a partial element equivalent circuit (PEEC) model. The issues associated with the order of the AWE approximation and calculation of the system response for these types of circuits are addressed. AWE calculations are compared to SPICE^{TM} calculations and published data where available.

INTRODUCTION

The electronics industry is placing more and more emphasis on design of electrical interconnects. This is in part due to the increasing clock frequencies and signal transients containing significant high frequency components. Parasitics produced by the interconnects can limit the overall system performance. Accurate models incorporating the parasitic phenomena are necessary tools for development of high speed systems.

Accurate computational modeling of electrical interconnects is often difficult to achieve. Circuits with seemingly simple geometries often require computationally complex algorithms due to the inhomogeneity of the layout. Lumped circuit analysis and transmission line theory can be used in many instances where the interconnect lines are parallel or connected to lumped circuit models. These techniques have the advantage that the same model can be used in the frequency domain or the time domain. Method of moments (MOM) analysis can be used in the frequency domain. The method of moments does not require the lines to be parallel. The computational overhead associated with method of moments analysis often limits the technique to simple geometries. The presence of a finite ground plane also greatly increases the complexity of the MOM solution. The finite-difference time-domain (FDTD) method can be used to analyze inhomogeneous geometries but the method can require a large amount of CPU time for circuit simulation.

When considering circuit models, the simplest method for analyzing electrical interconnects is to represent the circuit with an RC-tree model. RC-tree models can be used for estimating interconnect delay. They are not adequate for high speed applications where the mutual inductances and capacitances are significant. The next step up in complexity is to use lumped-pi or lumped-tee models which are limited to electrically short lines. A slightly more complex method is to use transmission line analysis. Transmission line analysis is valid for electrically long interconnects. In cases where the interconnects (or portions of the interconnect) are not parallel, the partial element equivalent circuit (PEEC) modeling method can be used to supplement or replace transmission line analysis [1, 2, 3]. In the PEEC modeling method, the interconnect is broken into small segments that are each represented by equivalent lumped circuit models.

Circuit analysis codes such as SPICE can be used to evaluate the circuit models. Large problems (many nodes) can require a great deal of CPU time for time-domain analysis. The PEEC models, for example, can be quite large, including several hundred inductances, capacitances and resistances. Asymptotic waveform evaluation (AWE) is a recently developed technique for efficient time-domain analysis of electrical interconnects [4, 5, 6]. The responses of large systems are asymptotically approximated with lower-order transfer functions. The transfer function for a large network is primarily dependent on the dominant system poles and corresponding residues. The AWE method extracts approximations to these dominant poles and residues through use of the Padé approximation and, hence, provides an accurate approximation of the system response. The AWE technique has been used to solve networks with RC trees, lumped elements, lossy coupled transmission lines, PEEC networks and nonlinear terminations [4, 5, 6, 7, 8, 9].

In this paper, the problem of using asymptotic waveform evaluation in the time domain to evaluate electrical interconnects is addressed. The interconnects are modeled with a lumped-pi model, a transmission line model and a partial element equivalent circuit. The advantage to using AWE is computational efficiency when handling larger circuit models. Because AWE is an approximate technique, however, care must be taken to ensure accurate results. Issues concerning accuracy and stability for the interconnect modeling are discussed. The next section of this paper presents some background on the network formulation for the interconnect models, the AWE analysis method, and the PEEC modeling technique as implemented in this study. Time-domain results computed using AWE for the different modeling methods are compared to each other and to computed SPICE results. Frequency-domain data for the system response is also presented and helps provide additional insight into the accuracy of the AWE solutions.

NETWORK MODELING AND FORMULATION OF THE AWE SOLUTION

An electrical network can be described as a lumped linear network or distributed network or combination of both using the modified nodal admittance (MNA) technique [10]. If the network is composed of lumped elements only, the system model can be analyzed using

$$\boldsymbol{Y}\,\boldsymbol{V} = \boldsymbol{I} \tag{1}$$

This would be the form for a circuit with only lumped circuits and PEEC elements. For an interconnect network that includes lumped circuits, PEEC models or possibly transmission lines, each set of transmission lines is treated as a subnetwork. The system matrix description from (1) can be augmented to include the distributed components. For an impulse excitation, the system matrix is given by [5]

$$\boldsymbol{W}\frac{d\boldsymbol{z}(t)}{dt} + \boldsymbol{H}\boldsymbol{z}(t) + \sum_{k=1}^{N_s} \boldsymbol{D}_k \boldsymbol{i}_k(t) - \boldsymbol{b}\delta(t) = 0 \tag{2}$$

where $\boldsymbol{z}(t)$ is a vector of length n containing the node voltages and independent voltage sources, current sources and linear inductor currents; $\boldsymbol{W}$ and $\boldsymbol{H}$ are n x n lumped network matrices; $\boldsymbol{b}$ is a vector of length n depending on the voltage sources and current sources; $\boldsymbol{D}_k$ is a selector matrix that maps the currents $\boldsymbol{i}_k(t)$ entering a linear subnetwork into the space of the pi-network; N_s is the number of linear subnetworks. In this study, the linear subnetworks are multiconductor transmission lines (MTLs). If subnetworks are not present in a circuit, the summation (third term) from (2) is omitted.

When a subnetwork is a multiconductor transmission line, the $\boldsymbol{D}_k$ selection matrix contains references for currents entering and leaving the

0-7803-2573-7/95/0000-0080 $4.00 © 1995 IEEE

transmission lines. For an MTL with N conductors, one reference conductor and length d, the terminal voltages and currents can be expressed as [9]

$$\begin{bmatrix} \boldsymbol{V}(d,s) \\ \boldsymbol{I}(d,s) \end{bmatrix} = e^{(\boldsymbol{D}+s\boldsymbol{E})d} \begin{bmatrix} \boldsymbol{V}(0,s) \\ \boldsymbol{I}(0,s) \end{bmatrix} = \boldsymbol{T}(s) \begin{bmatrix} \boldsymbol{V}(0,s) \\ \boldsymbol{I}(0,s) \end{bmatrix} \tag{3}$$

where

$$\boldsymbol{D} = \begin{bmatrix} \boldsymbol{0} & -\boldsymbol{R} \\ -\boldsymbol{G} & \boldsymbol{0} \end{bmatrix} \qquad \boldsymbol{E} = \begin{bmatrix} \boldsymbol{0} & -\boldsymbol{C} \\ -\boldsymbol{L} & \boldsymbol{0} \end{bmatrix} \tag{4a,b}$$

$\boldsymbol{R}, \boldsymbol{G}$ are the per-unit-length (PUL) resistance and conductance matrices, respectively, and $\boldsymbol{L}, \boldsymbol{C}$ are the PUL inductance and capacitance matrices, respectively. The "$\boldsymbol{0}$" represents a submatrix containing zeros. The $\boldsymbol{T}(s)$ is the transmission line parameter matrix. For the *nth* subnetwork, (3) can be restated in terms of the near-end and far-end voltages and currents

$$\boldsymbol{T}_n(s) \begin{bmatrix} \boldsymbol{V}_{NE,n} \\ \boldsymbol{I}_{NE,n} \end{bmatrix} - \begin{bmatrix} \boldsymbol{V}_{FE,n} \\ \boldsymbol{I}_{FE,n} \end{bmatrix} = 0 \tag{5}$$

The Laplace-domain form of (2) and (5) can be combined in a single matrix system of equations $\boldsymbol{Y}(s)\boldsymbol{X}(s) = \boldsymbol{E}_S$ represented by

$$\left[\begin{array}{c|ccccccccc} \multicolumn{1}{c|}{\boldsymbol{A}} & \multicolumn{8}{c}{\boldsymbol{B}} \\ \hline 0 & -1 & T_1 & 0 & 0 & 0 & \cdots & 0 & 0 \\ 0 & 0 & 0 & -1 & T_2 & 0 & \cdots & 0 & 0 \\ \vdots & \vdots & \vdots & \vdots & \vdots & \vdots & & \vdots & \vdots \\ 0 & 0 & 0 & 0 & 0 & 0 & \cdots & 0 & 0 \\ 0 & 0 & 0 & 0 & 0 & 0 & \cdots & -1 & T_{Ns} \end{array}\right] \left[\begin{array}{c} V_{NC} \\ I_{NC} \\ V_{FE,1} \\ I_{FE,1} \\ V_{NE,1} \\ I_{NE,1} \\ V_{FE,2} \\ I_{FE,2} \\ V_{NE,2} \\ I_{NE,2} \\ \vdots \\ V_{FE,Ns} \\ I_{FE,Ns} \\ V_{NE,Ns} \\ I_{NE,Ns} \end{array}\right] = \left[\begin{array}{c} b \\ \hline 0 \\ \hline 0 \\ \hline 0 \\ \hline 0 \\ \vdots \\ 0 \end{array}\right] \tag{6}$$

The matrix $\boldsymbol{Y}$ is organized into two major blocks. The upper block contains the parameters for all lumped circuit elements. If the circuit has only lumped circuits and PEEC models, the system matrix from (6) reduces to the upper left block $\boldsymbol{A}$. If MTLs are present, the lower block is populated with the transmission line parameter matrices from (3). The block $\boldsymbol{B}$ defines the connection of the MTL nodes with the lumped parameters and sources. The "$\boldsymbol{0}$" submatrices have all zero elements. The "$-\boldsymbol{I}$" submatrices are identity matrices multiplied by -1. The top block in the vector of unknowns $\boldsymbol{X}$ contains all voltages and currents $\boldsymbol{V}_{NC}, \boldsymbol{I}_{NC}$ that have *No* Common connection or nodes with any of the MTLs. In the event that MTLs are present, the remaining unknowns in the vector are organized into successive far-end voltage and current vectors $\boldsymbol{V}_{FE,n}$, $\boldsymbol{I}_{FE,n}$ and near-end voltage and current vectors $\boldsymbol{V}_{NE,n}, \boldsymbol{I}_{NE,n}$ for the N_s multiconductor transmission line networks. The vector of knowns $\boldsymbol{E}_S$ is given by the sources attached to lumped circuits or transmission lines $\boldsymbol{b}$ from (2) supplemented by a column of zeros.

Approximating the System Response Using Asymptotic Waveform Evaluation

Equation (6) can be expanded in a Maclaurin series [9]

$$\begin{aligned} &\left(\boldsymbol{Y}_{[0]} + s\boldsymbol{Y}_{[1]} + s^2\boldsymbol{Y}_{[2]} + \cdots\right) \\ &\qquad \times \left(\boldsymbol{X}_{[0]} + s\boldsymbol{X}_{[1]} + s^2\boldsymbol{X}_{[2]} + \cdots\right) = \boldsymbol{E} \end{aligned} \tag{7}$$

Equating terms of like powers of s gives

$$\boldsymbol{Y}_{[0]}\,\boldsymbol{X}_{[0]} = \boldsymbol{E} \tag{8}$$

$$\boldsymbol{Y}_{[0]}\,\boldsymbol{X}_{[n]} = -\sum_{r=1}^{n} \boldsymbol{Y}_{[r]}\,\boldsymbol{X}_{[n-r]} \tag{9}$$

where

$$\boldsymbol{Y}_{[n]} = \frac{\left[\frac{\partial^n}{\partial s^n}\boldsymbol{Y}_{(s)}\right]_{s=0}}{n!} \tag{10}$$

For a linear network containing lumped and distributed elements, the moments are given by [9]

$$\boldsymbol{M}_{[0]} = \boldsymbol{Y}_{[0]}^{-1}\boldsymbol{E} \tag{11}$$

$$\boldsymbol{M}_{[1]} = \boldsymbol{Y}_{[0]}^{-1}\left[-\boldsymbol{Y}_{[1]}\,\boldsymbol{Y}_{[0]}^{-1}\boldsymbol{E}\right] \tag{12}$$

$$\boldsymbol{M}_{[n]} = \boldsymbol{Y}_{[0]}^{-1}\left[-\sum_{r=1}^{n} \boldsymbol{Y}_{[r]}\,\boldsymbol{M}_{[n-r]}\right] \tag{13}$$

For a network with involving only lumped elements, the higher moments are given by

$$\boldsymbol{M}_{[n]} = \boldsymbol{Y}_{[0]}^{-1}\left[-\boldsymbol{Y}_{[1]}\,\boldsymbol{M}_{[n-1]}\right] \tag{14}$$

as $\boldsymbol{Y}_{[r]} = 0$ for $r \geq 2$.

Using asymptotic waveform evaluation, the transient response of the MNA circuit model for the electrical interconnect is approximated by matching the first $2q-1$ moments of the exact solution to a lower q-order model [4, 5, 6]. A brief summary of the AWE formulation as it pertains to this study is presented below.

The Laplace solution can be approximated from the first few lower order moments through use of the Padé approximation [12]. From the jth row in the moment matrix $\boldsymbol{M}$, the lower order moments at node j are given by

$$m_0 = \left[\boldsymbol{M}_{[0]}\right]_j,\ m_1 = \left[\boldsymbol{M}_{[1]}\right]_j,\ \ldots,\ m_n = \left[\boldsymbol{M}_{[n]}\right]_j \tag{15}$$

Let the lower order solution for node j be given by $\left[\boldsymbol{X}^*(s)\right]_j$. The lower order solution determined using the Padé approximation is [12]

$$\left[\boldsymbol{X}^*(s)\right]_j = \frac{F_K(s)}{G_Q(s)} = \frac{c_K s^K + c_{K-1}s^{K-1} + \cdots + c_1 s + c_0}{a_Q s^Q + a_{Q-1}s^{Q-1} + \cdots + a_1 s + 1} \tag{16}$$

The $G_Q(s)$ is normalized so that $a_0 = 1$ [12]. The rational fraction will have a Maclaurin series expansion equal to the original series expansion out to Q terms. The coefficients for the polynomial in the denominator are found using [5]

$$\begin{bmatrix} m_{K-Q+1} & m_{K-Q+2} & \cdots & m_K \\ m_{K-Q+2} & m_{K-Q+3} & \cdots & m_{K+1} \\ \vdots & \vdots & \vdots & \vdots \\ m_K & m_{K+1} & \cdots & m_{K+Q-1} \end{bmatrix} \begin{bmatrix} a_Q \\ a_{Q-1} \\ \vdots \\ a_1 \end{bmatrix} = -\begin{bmatrix} m_{K+1} \\ m_{K+2} \\ \vdots \\ m_{K+Q} \end{bmatrix} \tag{17}$$

For distinct poles with $K < Q$, (16) can be expressed as

$$\left[\boldsymbol{X}^*(s)\right]_j = \hat{c} + \frac{k_1}{s-p_1} + \frac{k_2}{s-p_2} + \cdots + \frac{k_Q}{s-p_Q} \tag{18}$$

where the k_n and p_n are the approximate poles and residues and $\hat{c}$ is a constant (the case for poles that are not distinct is treated in [4]). The poles of the system are approximated by computing the roots of the characteristic equation $G_Q(s)$ from (16). For $K = Q-1$, the residues of $\left[\boldsymbol{X}^*(s)\right]_j$ from (16), (18) are determined using [4]

$$\begin{bmatrix} p_1^{-1} & p_2^{-1} & \cdots & p_Q^{-1} \\ p_1^{-2} & p_2^{-2} & \cdots & p_Q^{-2} \\ \vdots & \vdots & \vdots & \vdots \\ p_1^{-Q} & p_2^{-Q} & \cdots & p_Q^{-Q} \end{bmatrix} \begin{bmatrix} k_1 \\ k_2 \\ \vdots \\ k_Q \end{bmatrix} = -\begin{bmatrix} m_0 \\ m_1 \\ \vdots \\ m_{Q-1} \end{bmatrix} \tag{19}$$

The residues may also be computed directly from the Padé

approximation rational function (16). In this study, the numerical software MATLAB® was used to find the poles and residues.

Varying K and Q makes it possible to have many sets of poles and residues. Each of these sets could be used to approximate the transfer function. The criteria for selecting the set of optimal poles that give the best approximation are given in [13,14]. The skew of a set of poles is a measure of the scaled difference between a given moment and its approximation. The optimal poles and residues correspond to the set with minimum skew.

The coefficients of the numerator $F_K(s)$ from (16) can be computed using the moments and the a_q coefficients. However, the Padé approximation can generate erroneous right half plane poles. To avoid including the spurious poles, the poles and residues are calculated without first formulating $F_K(s)$. The transfer function is then rebuilt by including only the legitimate left half plane pole terms. The time-domain response can be computed directly from the legitimate poles and residues (without reconstructing the approximate frequency response) using (20) below.

The accuracy of the AWE approximation primarily depends on the order of the approximation Q and the accuracy of the pole calculations at the point of expansion. In the original formulation for AWE, the moments are generated from expansion at $s=0$ (Maclaurin series) or from $s=\infty$ (Laurent series). The accuracy of the transfer function at any point in the complex s-plane is inversely related to its distance from the point of expansion. The inaccuracy can be minimized by generating the moments by expanding at different points in the complex plane using complex frequency hopping (CFH) [9, 11]. For AWE implemented with CFH, the poles and residues obtained from the different sets of expansion points can be combined for a more accurate approximation of the transfer function. For most electrical interconnect networks, however, the majority of the dominant poles are found at lower frequencies near $s=0$ [11].

The frequency domain impulse response is used to provide the AWE approximation to the time-domain impulse response of the system. The time-domain impulse response of $X(s)$ can be approximated by taking the inverse Laplace transform of (18) giving [5]

$$[X^*(s)]_j = \sum_{n=1}^{q} k_n e^{p_n t} \tag{20}$$

For the results presented in this paper, the time response for a given source waveform is determined by numerically convolving the waveform with (20).

AWE ANALYSIS OF ELECTRICAL INTERCONNECTS

In this section, electrical interconnects are evaluated using lumped-pi models, transmission line models and PEEC models. The circuits are evaluated in the time domain using AWE and SPICE. The formulations for the MNA network matrices used to generate the network equations are detailed for each of the examples. The pole and residue calculations will be discussed for the examples. Frequency domain data are also presented to provide more insight into the AWE approximation.

Lumped-Pi Model of a Three-Conductor Ribbon Cable

The crosstalk for the three-wire ribbon cable from Fig. 1 is evaluated using lumped-pi analysis. The lumped-pi model is valid for interconnects that are electrically short ($\ell < 0.1\lambda$ which restricts the region of validity for lumped-pi modeling to about 15 MHz for this problem). This model was taken from [15]. Conductor 0 is the reference conductor and is modeled by its internal resistance only. Conductor 2 is the driver and 1 is the receptor. The length of the cable is 2 m. The wire radii are all 7.5 mils and the insulation thickness is 10 mils. The wire spacing is 50 mils. Skin effect is not considered and the wire per-unit-length (PUL) resistance is assumed to be the dc value r_{dc} = 0.19444 ohm/m.

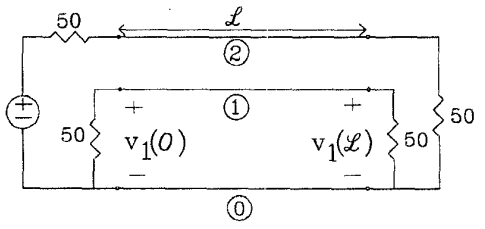

Figure 1. Circuit for the three-wire ribbon cable. The length is $\ell = 2$ m.

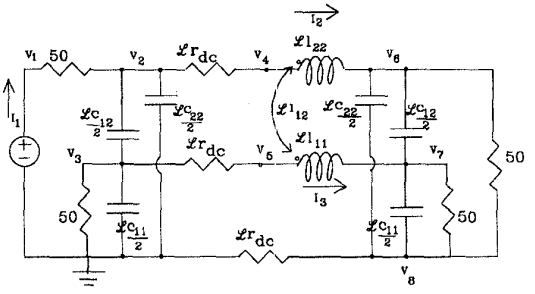

Figure 2. Lumped-pi model for the ribbon cable circuit shown in Fig. 1. The node numbers and current designations for the MNA matrix are shown.

The lumped-pi model for the circuit is shown above in Fig. 2. The inductance and capacitance matrices for this circuit are [15]

$$\boldsymbol{L} = \begin{bmatrix} 0.7485 & 0.5077 \\ 0.5077 & 1.0154 \end{bmatrix} \mu\text{H/m} \quad \boldsymbol{C} = \begin{bmatrix} 37.432 & -18.716 \\ -18.716 & 24.982 \end{bmatrix} \text{pF/m} \tag{21a,b}$$

The lumped-pi L_{ij}'s and C_{ij}'s are related to the elements of $\boldsymbol{L}$ and $\boldsymbol{C}$ multiplied by the total length ℓ [15]. The modified nodal admittance matrix is given by applying Kirchoff's current law at each node. The PUL parameters are scaled for improved matrix conditioning as outlined in [16]. The resistances are scaled to kohms, conductances to mS, inductances to μH, capacitances to pF, time in ns, frequency in GHz, voltages in V, and current in mA. The MNA equations are given by

$$\frac{(V_1 - V_2)}{50 \times 10^{-3}} - I_1 = 0 \quad , \qquad V_1 = 1 \tag{22a,b}$$

$$\frac{(V_2 - V_1)}{50 \times 10^{-3}} + \frac{(V_2 - V_4)}{\ell\, r_{dc}} + \frac{sC_{22}}{2} V_2 + \frac{sC_{12}}{2}(V_2 - V_3) = 0 \tag{22c}$$

$$\frac{V_3}{50 \times 10^{-3}} + \frac{(V_3 - V_5)}{\ell\, r_{dc}} + \frac{sC_{11}}{2} V_3 + \frac{sC_{12}}{2}(V_3 - V_2) = 0 \tag{22d}$$

$$\frac{(V_4 - V_2)}{\ell\, r_{dc}} - I_2 = 0 \quad , \qquad \frac{(V_5 - V_3)}{\ell\, r_{dc}} + I_3 = 0 \tag{22e,f}$$

$$\frac{(V_6 - V_8)}{50 \times 10^{-3}} + \frac{sC_{22}}{2}(V_6 - V_8) + \frac{sC_{12}}{2}(V_6 - V_7) - I_2 = 0 \tag{22g}$$

$$\frac{(V_7 - V_8)}{50 \times 10^{-3}} + \frac{sC_{11}}{2}(V_7 - V_8) + \frac{sC_{12}}{2}(V_7 - V_6) - I_3 = 0 \tag{22h}$$

$$\frac{(V_8 - V_7)}{50 \times 10^{-3}} + \frac{(V_8 - V_6)}{50 \times 10^{-3}} + \frac{sC_{11}}{2}(V_8 - V_7) + \frac{sC_{22}}{2}(V_8 - V_6) + \frac{V_8}{\ell\, r_{dc}} = 0 \tag{22i}$$

Additional equations are obtained by applying Kirchoff's voltage law at the two inductors giving

$$V_4 - V_6 - sL_{11}I_2 - sL_{12}I_3 = 0 \quad (23a)$$

$$V_5 - V_7 - sL_{12}I_2 - sL_{11}I_3 = 0 \quad (23b)$$

The system described by (22) and (23) can be represented by a matrix equation of the form (6). Only the upper-left block of the Y-matrix from (6) is required since there are only lumped elements in this example. From (8),

$$Y(0) = Y(s)\,|_{s=0} \quad (24)$$

which is the dc matrix. The first moment or the dc response is obtained from (11). Subsequent moments would be computed using (12) and (14).

The Padé approximation cannot extract more than approximately 8 to 10 stable poles from a Taylor series [9] and most of the signal is often found near $s = 0$. In this example, a $6th$-order approximation (6 poles) is computed. The system poles are extracted by substituting the moments from any node into (17) and determining the roots of the denominator of (16). The moment at node j can be obtained by selecting the jth row of the moment matrix.

The scaled poles computed using AWE closely matched the poles obtained through exact solution of the MNA equations (22) and (23). The exact poles and the poles computed using AWE are shown in Table I. Care must be exercised when computing the poles using AWE. AWE is an approximate technique and improper pole selection can lead to extraneous poles. For proper pole selection, several criteria are used [9,13,14]. There are 6 poles in this particular circuit. The set of poles corresponding to $K = 3$, $Q = 6$ from (16) provided for minimum skew.

Table I. Comparison of the exact poles of the lumped-pi model to those computed using AWE for the lumped-pi model.

Exact Poles, Lumped-pi	AWE poles, Lumped-pi
-1.7417e00	-1.7417e00
-1.7050e00	-1.7051e00
-3.9269e-01	-3.9269e-01
-1.9667e-01+ i 1.2861e-01	-1.9667e-01- i 1.2861e-01
-1.9667e-01- i 1.2861e-01	-1.9667e-01+ i 1.2861e-01
-3.6723e-02	-3.6723e-02

The near end crosstalk is obtained by computing the residues using the moments of the $3rd$ node. Once the poles and residues are computed, the impulse response is found using (20). The MATLAB "lsim"-function was used to compute the time domain response.

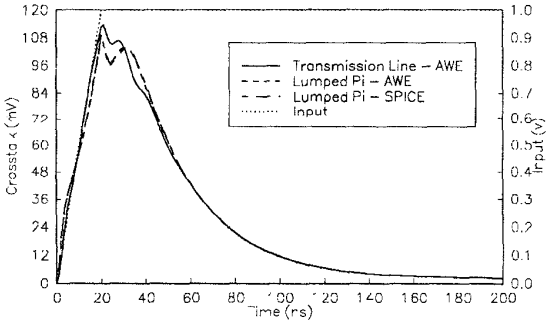

Figure 3. Time-domain near-end crosstalk for the three-conductor circuit of Fig. 1. The results are for node 3 in Fig. 2. The input waveform is a pulse with a 20 ns rise time.

Figure 3 above shows the response to a pulse that has 20 ns rise time. The AWE results match very closely with the results generated using a SPICE simulation. The frequency domain response of the AWE approximation can also be computed using (18). The magnitude and phase of the frequency response is shown in Fig's. 4 and 5.

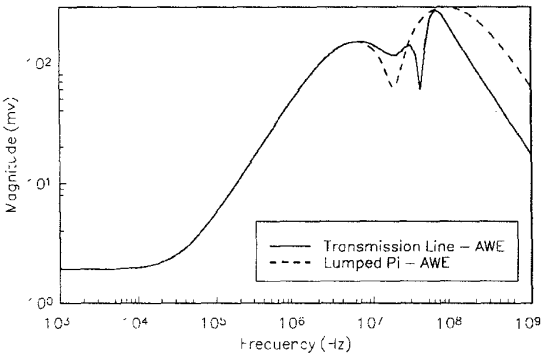

Figure 4. Magnitude of the frequency-domain representation of the impulse response at the near-end of the receptor circuit for the three-conductor circuit of Fig. 1. The transmission line model is valid for higher frequencies.

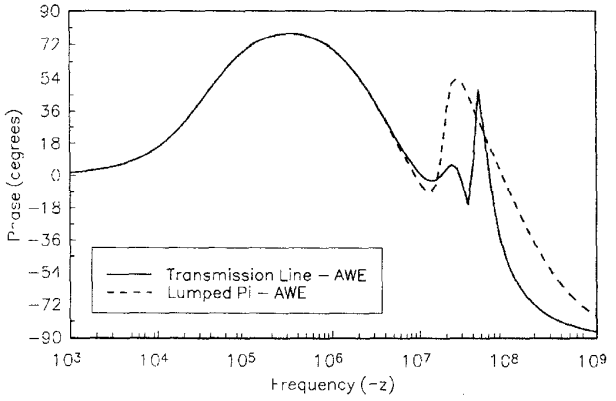

Figure 5. Phase of the frequency-domain representation of the impulse response at the near-end of the receptor circuit for the three-conductor circuit of Fig. 1. The transmission line model is valid for higher frequencies.

Transmission Line Model of a Three-Conductor Ribbon Cable

The lumped-pi model of the circuit from Fig. 1 is valid only at lower frequencies where the length of the transmission line is short compared to a wavelength at the highest frequency of interest. Transmission line (TL) theory can be used to model the circuit when the length is electrically significant. The TL model for the circuit is shown in Fig. 6. The lines are modeled using distributed parameters while the sources and loads are modeled using lumped elements. The MNA equations are written in terms of the node voltages and the voltages and currents at the near and far ends of the transmission lines. The source and load equations are found through application of Kirchoff's current law at each node.

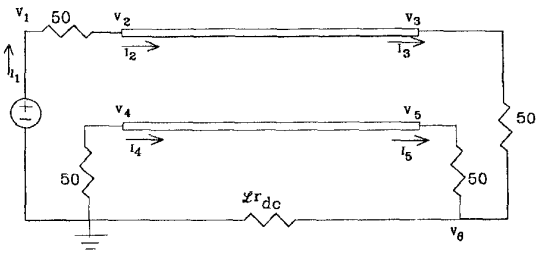

Figure 6. Transmission line model for the circuit from Fig. 1.

The transmission line relationships are given by

$$\begin{bmatrix} V_3(s) \\ V_5(s) \\ I_3(s) \\ I_5(s) \end{bmatrix} = e^{(D+sE)d} \begin{bmatrix} V_2(s) \\ V_4(s) \\ I_2(s) \\ I_4(s) \end{bmatrix} \tag{25}$$

where

$$\boldsymbol{R} = \begin{bmatrix} r_{dc} & 0 \\ 0 & r_{dc} \end{bmatrix} \tag{26}$$

$\boldsymbol{L}$ and $\boldsymbol{C}$ are given by (21a,b). For this problem, the $\boldsymbol{G}$ matrix elements are all zero. The exponential matrix from (25) can be expressed as (upon factoring into like powers of s)[9]

$$\begin{aligned} e^{(D+sE)d} &= \left[I + Dd + \frac{D^2d^2}{2!} + \cdots \right] \\ &+ s\left[Ed + \frac{1}{2!}(DE+ED)\, d^2 + \frac{1}{3!}(D^2E+DED+ED^2)\, d^3 + \cdots \right] \\ &+ s^2\left[\frac{1}{2!}E^2d^2 + \frac{1}{3!}(DE^2+EDE+E^2D)\, d^3 + \cdots \right] + \cdots \end{aligned} \tag{27}$$

Substituting the expansion of (27) into the MNA from (6) and following the moment generation steps shown in the case of the lumped-pi model, the moments can be computed. At $s=0$, the 4 transmission line equations of the $\boldsymbol{Y}$-matrix reduce to

$$\begin{bmatrix} V_3 \\ V_5 \\ I_3 \\ I_5 \end{bmatrix} = \left[I + Dd + \frac{D^2d^2}{2!} + \cdots \right] \begin{bmatrix} V_2 \\ V_4 \\ I_2 \\ I_4 \end{bmatrix} \Bigg|_{s=0} \tag{28}$$

For $\boldsymbol{Y}_{[1]}$ and the remaining Maclaurin series' $\boldsymbol{Y}$-matrices, the elements of the first 7 rows are all zero as there are no capacitances or inductances in the lumped element description of the MNA equations. The last 4 rows are given by the derivatives of the exponential

$$\boldsymbol{Y}_{[n]_{\text{rows7:11}}} = \frac{\partial^n}{\partial s^n} e^{(D+sE)d} \Big|_{s=0} \tag{29}$$

For example,

$$\begin{aligned} \boldsymbol{Y}_{[1]_{\text{rows7:11}}} &= Ed + \frac{1}{2!}(DE + ED)\, d^2 \\ &+ \frac{1}{3!}(D^2E + DED + ED^2)\, d^3 + \cdots \end{aligned} \tag{30}$$

A *6th*-order AWE approximation was performed for the transmission line structure of Fig. 6. The poles and residues are obtained from the moments of nodes 3 and 4. The set of poles corresponding to $K=3, Q=6$ from (16) provided for minimum skew. The time-domain near end crosstalk is computed and is shown in Fig. 3 along with the lumped-pi results. The frequency-domain results are shown in Fig's. 4 and 5.

Increasing the order of the approximation increases the frequency range over which the AWE approximation gives accurate results. In theory, the transmission line formulation has infinite bandwidth. The order of approximation required for a particular problem depends on the application. The lower poles affect the slowly varying time-domain characteristics (such as dc levels) while the upper poles affect the rapidly-varying time-domain (sharp edges). When considering radiated emissions, the upper poles correspond to the higher-frequency radiated field components.

A comparison of the effects of varying the order of approximation is shown in Fig's. 7 and 8. The transmission line structure from Fig. 6 was used for the comparison. The order of the approximation was increased from 2 poles to 6 poles. In Fig. 7, the frequency-domain representation of the impulse response at the near-end of the receptor circuit is shown. Increasing the number of poles improves the accuracy of the approximation at the higher frequencies. The effects for the time-domain crosstalk are shown in Fig. 8. A simple second-order approximation is sufficient if a reasonable estimate of the peak of the crosstalk waveform is all that is required. Increasing the order of the approximation adds the rapidly-varying details to the waveforms.

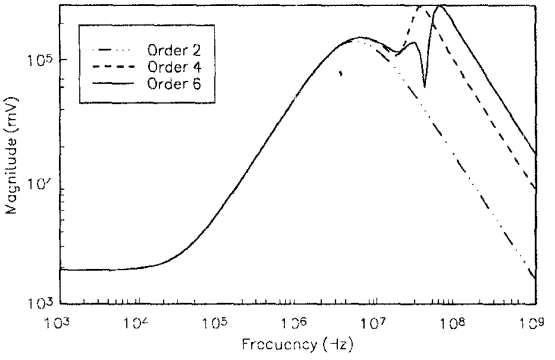

Figure 7. Frequency-domain representation of the impulse response at the near-end of the receptor circuit for the transmission line from Fig. 6. The order of the AWE approximation is increased to illustrate the effects on the frequency response.

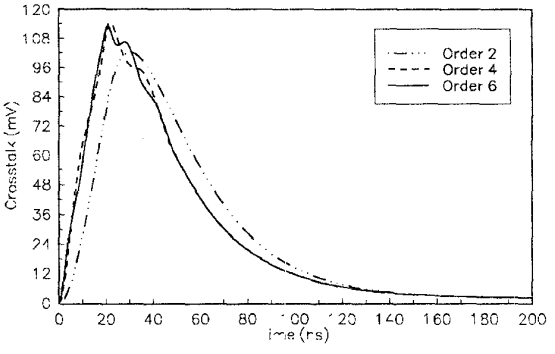

Figure 8. Time-domain near-end crosstalk for the transmission line circuit from Fig. 6. The order of the AWE approximation is increased to illustrate the effects on the time response.

PEEC Analysis of a Three-Conductor Circuit

Transmission line circuits can be modeled with lumped-pi analysis assuming the size of the circuits is small compared to a wavelength. Transmission line theory can be used when the conductors are parallel and their length is significant relative to a wavelength. Transmission line models are formulated through the use of per-unit-length parameters that are computed assuming a two-dimensional structure and TEM wave behavior. Transmission line models effectively have no upper frequency limit due to the two dimensional assumptions. In actual finite length interconnects, the 3-D effects can be effectively accounted for through use of partial element equivalent circuits (PEEC) [17].

A lossless, three-conductor printed circuit is shown in Fig. 9.The conductors are divided into multiple segments as shown in Fig. 10. Each conductor was divided into 16 segments and the partial inductances and capacitances were computed. The Y-matrix is a 95x95 array. It is similar to the matrix of a lumped circuit model as the transmission lines are modeled using discrete segments and not distributed parameters as was done for the above transmission line model. There are 49 node voltages, 1 source (I_1) and 45 inductor currents (I_2 through I_{46}). The input pulse has a 20 ns rise time. A 4*th* order AWE approximation was formulated for this PEEC problem. The set of poles corresponding to $K = 3$, $Q = 4$ from (16) provided for minimum skew. The near end crosstalk computed using AWE is compared to the SPICE simulation using a lumped-pi model of the 3 conductor circuit (see Fig. 11).

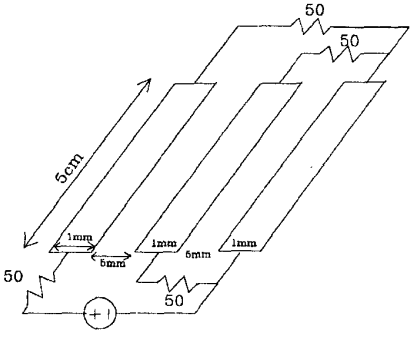

Figure 9. Lossless, three-conductor printed circuit used for PEEC analysis.

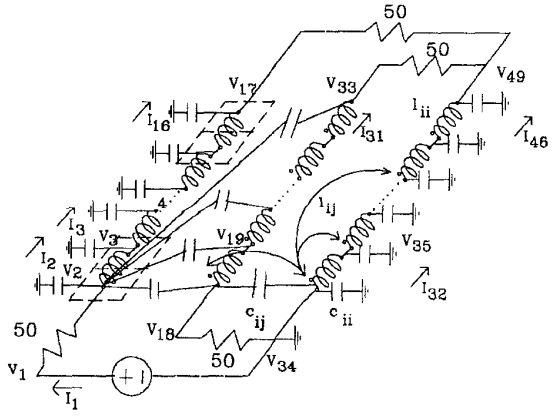

Figure 10. Illustration of the model generated for the three-conductor circuit from Fig. 7 using PEEC segmentation.

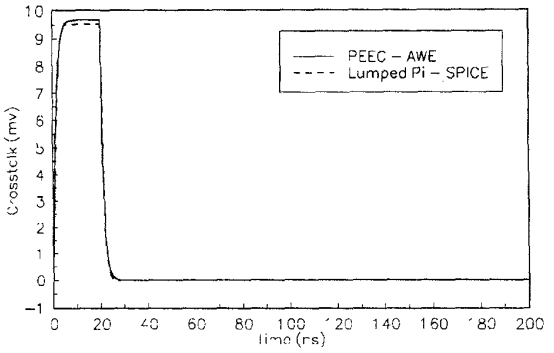

Figure 11. Time-domain near-end crosstalk computed for the circuit from Fig. 7. The input waveform is a pulse with a 20 ns rise time.

REFERENCES

1.A. E. Ruehli, "Equivalent Circuit Models for Three-Dimensional Multiconductor Systems," *IEEE Trans. Microwave Theory Tech.*, vol. 22, no. 3, pp. 216-221, March, 1974.

2.A. E. Ruehli, "Inductance Calculations in a Complex Integrated Circuit Environment," *IBM J. Res. Develop.*, pp. 470-481, September, 1972.

3.A. E. Ruehli, P. A. Brennan, "Efficient Capacitance Calculations for Three Dimensional Multiconductor Systems," *IEEE Trans. Microwave Theory Tech.*, vol. 21, no. 2, pp. 76-82 February, 1973.

4.L. T. Pillage, R. A. Rohrer, "Asymptotic Waveform Evaluation for Timing Analysis," *IEEE Trans. Computer Aided-Design*, vol. 9, no. 4, pp. 352-366, April, 1990.

5.T. K. Tang, M. S. Nakhla, "Analysis of High-Speed VLSI Interconnects Using the Asymptotic Waveform Evaluation Technique," *IEEE Trans. Computer-Aided Design*, vol. 11, no. 3, pp. 341-352, March, 1992.

6.J. E. Bracken, V. Raghavan, R. A. Rohrer, "Interconnect Simulation with Asymptotic Waveform Evaluation (AWE)," *IEEE Trans. Circuits and Systems*, vol. 39, pp. 869-878, November, 1992.

7.H. Heeb, A. E. Ruehli, J. E. Bracken, R. A. Rohrer, "Three Dimensional Circuit Oriented Electromagnetic Modeling for VLSI Interconnects," *Proc. of IEEE Int. Conf. on Computer Design*, pp. 218-221, 1992.

8.D. Xie, M. S. Nakhla, "Delay and Crosstalk Simulation of High-Speed VLSI Interconnects with Nonlinear Terminations," IEEE Trans. Computer Aided Design, vol. 12, pp. 1198-1211, November, 1993.

9.E. Chiprout, M. S. Nakhla, Asymptotic Waveform Evaluation and Moment Matching for Interconnect Analysis, Kluwer Academic Publishers, Boston, 1994.

10.C. W. Ho, A. E. Ruehli, P. A. Brennan, "The Modified Nodal Approach to Network Analysis," *IEEE Trans. Circuits Syst.*, vol. CAS-22, pp. 504-509, June, 1975.

11.E. Chiprout, M. S. Nakhla, "Analysis of Interconnect Networks Using Complex Frequency Hopping (CFH)," accepted for publication.

12.G. A. Baker, Jr., P. Graves-Morris, *Padé Approximants, Part I: Basic Theory*, Addison-Wesley Publishing Company, Reading, Massachusetts, 1981.

13.E. Chiprout, M. S. Nakhla, "Generalized Moment-Matching Methods for Transient Analysis of Interconnect Networks," *29th ACM/IEEE Design Automation Conference*, Anaheim, pp. 201-206, June, 1992.

14.E. Chiprout, M. S. Nakhla, "Optimal Pole Selection in Asymptotic Waveform Evaluation," *Proceedings of the IEEE International Symposium on Circuits and Systems*, San Diego, pp. 1961-1964, May, 1992.

15.C. R. Paul, Analysis of Multiconductor Transmission Lines, John Wiley and Sons, New York, 1994.

16.J. Vlach, K. Singhal, Computer Methods for Circuit Analysis and Design, Van Nostrand Reinhold, New York, 1983.

17.E. Chiprout, H. Heeb, M. S. Nakhla, A. E. Ruehli, "Simultaneous 3-D Retarded Interconnect Models Using Complex Frequency Hopping (CFH)," *IEEE Int. Conf. on Computer Aided Design*, pp. 66-72, November, 1993.